HHS Public Access

Author manuscript

J Mol Cell Cardiol. Author manuscript; available in PMC 2020 March 01.

Published in final edited form as:

J Mol Cell Cardiol. 2019 March ; 128: 51–61. doi:10.1016/j.yjmcc.2019.01.013.

Acute AT_1R blockade prevents isoproterenol-induced injury in *mdx* hearts

Tatyana A. Meyers[a], **Jackie A. Heitzman**[a], **Aimee Krebsbach**[a,b], **Lauren M. Aufdembrink**[a], **Robert Hughes**[a], **Alessandro Bartolomucci**[a], and **DeWayne Townsend**[a,b,*]

[a]Department of Integrative Biology and Physiology, University of Minnesota Medical School, Minneapolis, MN, USA

[b]Lillehei Heart Institute, University of Minnesota Medical School, Minneapolis, MN, USA

Abstract

Background: Duchenne muscular dystrophy (DMD) is an X-linked disease characterized by skeletal muscle degeneration and a significant cardiomyopathy secondary to cardiomyocyte damage and myocardial loss. The molecular basis of DMD lies in the absence of the protein dystrophin, which plays critical roles in mechanical membrane integrity and protein localization at the sarcolemma. A popular mouse model of DMD is the mdx mouse, which lacks dystrophin and displays mild cardiac and skeletal pathology that can be exacerbated to advance the disease state. In clinical and pre-clinical studies of DMD, angiotensin signaling pathways have emerged as therapeutic targets due to their adverse influence on muscle remodeling and oxidative stress. Here we aim to establish a physiologically relevant cardiac injury model in the mdx mouse, and determine whether acute blockade of the angiotensin II type 1 receptor (AT_1R) may be utilized for prevention of dystrophic injury.

Methods and Results: A single IP injection of isoproterenol (Iso, 10 mg/kg) was used to induce cardiac stress and injury in mdx and wild type (C57Bl/10) mice. Mice were euthanized 8 hours, 30 hours, 1 week, or 1 month following the injection, and hearts were harvested for injury evaluation. At 8 and 30 hours post-injury, mdx hearts showed 2.2-fold greater serum cTnI content and 3-fold more extensive injury than wild type hearts. Analysis of hearts 1 week and 1 month after injury revealed significantly higher fibrosis in mdx hearts, with a more robust and longer-lasting immune response compared to wild type hearts. In the 30-hour group, losartan treatment initiated 1 hour before Iso injection protected dystrophic hearts from cardiac damage, reducing mdx acute injury area by 2.8-fold, without any significant effect on injury in wild type hearts. However, both wild type and dystrophic hearts showed a 2-fold reduction in the magnitude of the macrophage response to injury 30 hours after Iso with losartan.

*Correspondence directed to: Department of Integrative Biology and Physiology, Medical School, University of Minnesota, 2231 6th Street SE, Minneapolis, MN 55455.

Declarations of interest: none

Conclusions: This work demonstrates that acute blockade of AT_1R has the potential for robust injury prevention in a model of Iso-induced dystrophic heart injury. In addition to selectively limiting dystrophic cardiac damage, blocking AT_1R may serve to limit the inflammatory nature of the immune response injury in all hearts. Our findings strongly suggest that earlier adoption of angiotensin receptor blockers in DMD patients could limit myocardial damage and subsequent cardiomyopathy.

Keywords

Duchenne muscular dystrophy; dystrophic cardiomyopathy; fibrosis; angiotensin; immune infiltration

1. INTRODUCTION

Muscular dystrophies are a genetically diverse group of rare muscle wasting diseases that often involve the heart, resulting in clinically significant cardiomyopathy [1–5]. Duchenne muscular dystrophy (DMD) is the most common form, having an X-linked inheritance pattern with an incidence of roughly 1 in every 3,500-5,000 boys [3,6]. The molecular basis of DMD lies in the loss of the protein dystrophin, which normally plays a critical role in maintaining the membrane integrity of muscle cells by serving as a molecular link between the cytoskeleton and the extracellular matrix and a signaling scaffold at the sarcolemma [7–11]. Dystrophin loss results in myocyte necrosis, replacement of myocytes with extensive fibrosis, and eventual loss of muscle mass [12,13]. Clinically, DMD is characterized by rapidly progressing skeletal muscle wasting, loss of ambulation and other motor functions, respiratory insufficiency, and pronounced heart disease [2,3,14]. As improvements in symptomatic respiratory therapies have prolonged patient life spans, heart failure is becoming a more common cause of premature death in patients with muscular dystrophy [1,15,16].

The *mdx* mouse is a commonly-used preclinical model of DMD, having a spontaneous mutation in the DMD locus that results in the absence of dystrophin [7,17,18]. In young adulthood, its disease is mild, but investigators have successfully used aged mice, exogenous stressors, or additional genetic manipulations to advance the disease state [3,19–26]. Multiple studies aimed at modulating the mdx phenotype have pointed to angiotensin-related signaling pathways and oxidative stress as important factors in both the skeletal and cardiac phenotype of dystrophic mice [26–31]. Importantly, drugs including ACE inhibitors (ACEi), angiotensin receptor blockers (ARBs), and antioxidants have shown a significant benefit for dystrophic mice and human patients [22,32–38]. Current recommendations guide clinicians to consider initiating ACEi or ARB therapy at the age of 10 in Duchenne patients even without cardiac symptoms. This recommendation is grounded in the thought that these drugs help primarily by minimizing adverse remodeling following cardiomyocyte loss [2,3]. However, if these drugs are able to limit cardiomyocyte loss, initiation at the age of 10 may be too late, as patients may already be losing myocardium well before this point [1,39–41].

Our group and others have used adrenergic agonists like isoproterenol (Iso) and dobutamine to stress mdx hearts to better recapitulate the severity of the human cardiac pathology

[23,24,42,43]. Iso is a selective agonist of all β-adrenergic receptor isoforms that drives a sharp increase in heart rate and cardiac contractility [44], producing a sufficiently high workload to damage membranes of susceptible cardiomyocytes. This model has advantages over further genetic manipulation or aging by reducing confounding factors and allowing for more direct comparisons to other literature featuring adult mdx mice. Additionally, this adrenergic stress model may be particularly relevant to the perioperative stresses faced by Duchenne patients, whose treatment course may include procedures requiring anesthesia, such as scoliosis correction or fracture repair, that may result in bouts of elevated cardiac stress [2,45].

In the present study, we evaluate the cardiac consequences of a single bolus of Iso in the mdx mouse, and combine this Iso-mediated cardiac insult with acute losartan treatment to evaluate the potential benefits of ARB therapy for cardiomyocyte survival. These data reveal an interaction between workload-induced cardiac injury and exacerbation of this injury downstream of angiotensin II type 1 receptor (AT_1R) in dystrophic hearts, showing a significant reduction in acute myocardial damage with ARB treatment at the time of Iso-induced cardiac stress. The potential cardiac protection and good overall tolerability suggest that early initiation of ARB therapy may provide a readily available means to slow the onset of dystrophic cardiomyopathy.

2. METHODS

2.1. Animals

The wild type control strain C57BL/10SnJ (C10) and the dystrophic strain C57BL/10ScSn-Dmd^{mdx}/J(mdx) were bred and maintained at the University of Minnesota from breed stock obtained from Jackson Laboratories (Bar Harbor, ME). To limit genetic drift within this colony, breed stock were purchased from Jackson Laboratories every 5-6 generations. All mice were 4-6 months of age at the time of experiments and were housed in static (non-ventilated) cages with a 12-hour light-dark cycle. As DMD is a disease predominantly affecting males, only male mice were used in these studies. All animal procedures were approved by the University of Minnesota Institutional Animal Care and Use Committee and performed in compliance with all relevant laws and regulations.

2.2. Isoproterenol studies

(−)-Isoproterenol hydrochloride (Iso; Sigma #I6504) was dissolved in saline and sterile filtered into a foil-wrapped red-top glass vial prior to injection. The sterile Iso solution was stored at 4°C for no more than 3 days, and any solution developing discoloration, indicative of degradation, was discarded. Mice received a single IP bolus injection of 10 mg/kg Iso in volumes of 40-70 μl adjusted for body weight. Hearts were harvested at timepoints of 8 hours, 30 hours, 1 week, and 1 month after the injection (Fig. 1A).

2.3. Serum cTnI measurements

For a subset of mice, blood was collected from the facial vein of isoflurane-anesthetized mice 1 week prior to the Iso injection for the baseline serum cTnI measurement, and again 8 hours following the Iso injection. The collected blood was allowed to clot on ice, then spun

to separate the serum, which was then stored at −80°C until analysis. Serum cardiac troponin I content (cTnI) was measured via a cTnI test kit on the Stratus CS Stat fluorometric analyzer (Siemens Healthcare).

2.4 Losartan studies

An additional subset of mice was assigned to receive losartan 1 hour prior to and alongside Iso, terminating at the 30-hour timepoint. Losartan solution was made on the day prior to Iso injections from a crushed generic losartan tablet (100mg) dissolved in saline to a final concentration of 6 mg/ml, and sterile filtered. Doses were calculated based on mouse body weights, the injection schedule, and the pharmacokinetics of losartan as well as its primary active metabolite EXP3174 [46,47]. At the start of the light cycle on the day of the study, the mice received a loading dose in the form of a 60 mg/kg losartan bolus injection, followed a single 10mg/kg Iso injection 1 hour later, and a 20 mg/kg losartan booster 6 hours after the first bolus. At the end of the light cycle, the mice received another bolus of 60 mg/kg losartan to span the dark cycle. At the end of the dark cycle, they received a final booster of 20 mg/kg losartan, and hearts were harvested 7 hours later (30 hours from the Iso bolus). This dosing regimen was based on the half-lives of losartan and its major active metabolite, and intended to minimize the troughs in drug serum levels after the loading dose without disruptions to the dark cycle.

2.5. Histopathology

Fresh excised hearts were rinsed in PBS and cut in half along the transverse plane. The apical half was placed into OCT medium inside a block mold, and the OCT block was frozen in liquid nitrogen-cooled isopentane. Heart block sections were cut to 7 microns and placed on plus slides to be stained. Slides used for dystrophin and actinin staining were fixed in cold acetone for 10 minutes before rehydration and staining, while all other immunofluorescent staining was performed on unfixed slides. The following antibodies and reagents were used for IF staining: goat serum for blocking (Jackson ImmunoResearch# 005-000-121, 10%), rabbit actinin polyclonal antibody (Novus #NBP1-32462, 1:150), rabbit dystrophin polyclonal antibody (Abeam #ab15277, 1:150), rat AlexaFluor 488 anti-mouse CD68 antibody – clone FA-11 (Biolegend, 1:150), rat AlexaFluor 647 anti-mouse CD45 antibody – clone 30-F11 (Biolegend, 1:100), goat anti-mouse IgG (H+L) secondary antibody (Invitrogen #R37121, 1:200), goat anti-rabbit IgG (H+L) secondary antibody (Invitrogen #A-11008, 1:200), WGA AlexaFluor conjugate (ThermoFisher, 5μg/ml), and ProLong Gold Antifade Mountant with DAPI (ThermoFisher). All immunofluorescence incubation steps were carried out at room temperature for 1 hour, separated by three 5-minute washes in fresh PBS. The following reagents were used for Sirius Red Fast Green (SRFG) staining: 1.2% picric acid solution (Ricca #R5860000), Direct Red 80 (Sigma #365548), Fast Green FCF (Sigma #F7252), Formula 83 clearing solvent (CBG Biotech F83), and organic mounting medium (CBG Biotech MM83). Prior to SRFG staining via a modified protocol based previously described methods [20], slides were fixed for 3 hours in cold acetone, and rehydrated in 70% ethanol followed by tap water. The tissue was then stained for 25 minutes in SRFG dye solution of picric acid, 0.1% Direct Red 80, and 0.1% Fast Green FCF, followed by washes in tap water and dehydration in 70% ethanol, 100% ethanol, and Formula 83.

2.6. Microscopy

All imaging was performed in NIS Elements software on a Nikon Eclipse Ni-U upright epifluorescent microscope with motorized stage and filter wheel. For cell infiltration and acute lesion studies, whole heart montages were collected as a stack of three to four fluorescent channels at a resolution of 0.92 μm/pixel. For fibrosis studies, SRFG-stained sections were collected as brightfield montages at a resolution of 0.85 μm/pixel. For assessment of birefringence, images with a resolution of 0.17 μm/pixel were collected using orthogonally oriented polarized filters flanking the slide. Dystrophin and actinin IF close-up images were collected at a resolution of 0.23 μm/pixel, and deconvolved via the automatic 2D deconvolution package in NIS Elements.

2.7. Image analysis

All images were analyzed under deidentified names in a blinded fashion in Fiji using custom macros and scripts. IgG analysis was carried out using 1180×944 μm (1280×1024 pixels) non-overlapping frames taken from whole montages to minimize complications arising from variations in brightness across the whole heart section. IgG lesion area was determined by thresholding the IgG image for total lesion area (indicated by bright IgG-positive signal) and dividing that by total heart section area (provided by tissue autofluorescence). Fibrosis analysis of SRFG-stained sections was carried out on entire heart montages using the color threshold function in Fiji. Areas containing collagen, which takes up Sirius Red dye, were identified by measuring the pixel area corresponding to a red hue. The fibrotic area was then divided by total heart pixel area, corresponding to any hue and saturation that exceeds the neutral background.

Birefringence analysis was carried out using 2360×1770 μm (2560×1920 pixels) frames imaged using brightfield, and matching frames imaged with orthogonally oriented polarized filters flanking the slide. Total birefringent area was calculated as the number of pixels corresponding to a signal that exceeds the brightness of the surrounding myocardium. The birefringent area was divided by the total red area from the matched brightfield image to calculate the percent birefringence of each fibrotic lesion.

Cell infiltration analysis workflow began with a blinded scrubbing of IF montage images in which artifacts were removed, including blood within the ventricles or large vessels, non-specific aggregates of dye, and areas in which the tissue was folded. Lesion-positive regions and total muscle area were determined by thresholding the entire montage, followed by a manual removal or addition of misidentified areas. Cell-specific thresholds were set to identify cell-positive regions, which were then compared to the lesion areas. Any cell-positive region containing a shared pixel with a lesion was considered a lesion-positive cell region. Results represent the percentage of cell-positive pixels relative to the total number of heart pixels. All data analysis scripts were performed in FIJI and R.

2.7. Statistics

Statistical analyses were performed using Prism 7 (GraphPad Software) and R [48]. Statistical comparisons were made using one-way ANOVA or two-way ANOVA where

appropriate, with Sidak multiple comparison post-hoc test to identify specific differences between relevant groups. All column and line graphs display the mean ± standard error.

3. RESULTS

3.1. A single dose of isoproterenol causes acute myocardial injury that is significantly exacerbated in dystrophic hearts.

Within hours of injection of a single dose of isoproterenol (Iso), areas of acute myocardial injury could be identified by staining for myocyte infiltration of endogenous IgG. The accumulation of intracellular IgG is only expected to occur in myocytes whose membranes have been sufficiently disrupted to become permeable to large molecules like serum proteins. Quantification of acute myocardial damage revealed that injured myocyte area is already prominent as early 8 hours, with a peak at 30 hours after Iso administration. This acute injury is completely removed 1 week after the Iso injection (Fig. 1B). A significant difference was found between healthy and dystrophic hearts at the 30-hour timepoint, with mdx hearts showing 3-fold greater injury than that seen in wild type hearts (18.9±2.8% versus 6.3±1.7%, respectively).

Examination of entire heart montages revealed that in dystrophic hearts, these acute lesions were large and scattered throughout the whole heart section. In contrast, acute injury in wild type hearts manifested as smaller lesions that were concentrated in the endocardium (Fig. 1C). This hints that the Iso-induced injury in C10 hearts may result from perfusion-demand mismatching, with relative hypoperfusion of the endocardium during Iso-induced increases if cardiac workload resulting in myocardial injury. This mechanism is likely also active in the dystrophic heart, but large swaths of injured myocardium are also found throughout the rest of the heart, suggesting an additional mechanism of injury is at play. Mice with genetic ablation of all β-adrenergic receptors showed no functional or histological response to the dose of Iso used in these studies (data not shown), confirming the β-adrenergic receptor specificity of Iso action.

3.2. Isoproterenol-induced sarcolemmal injury triggers cardiomyocyte destruction.

Closer inspection of the regions of acute injury revealed multiple signs of myocyte degeneration at 8 hours after Iso injection. In intact myocytes, sarcomeric α-actinin was localized in a pattern of orderly striations, but within IgG^+ myocytes it displayed a marked disruption of this striated pattern (Fig. 2A). Signs of myocyte breakdown are not limited to the degradation of the contractile apparatus, as dystrophin staining at the membrane was also largely lost in injured wild type myocytes (Fig. 2B). The loss of normal sarcomeric patterning and sub-membrane protein localization suggests that these damaged myocytes are undergoing widespread proteolysis. No qualitative differences in the myocyte degradation process were found between injured areas in wild type and dystrophic hearts at 8 or 30 hours after Iso administration.

Serum cardiac troponin (cTn) content is an index of cardiomyocyte integrity, and elevated cTnI and cTnT levels have been documented in boys with DMD [49–52]. Untreated adult dystrophic mice showed no detectable ongoing basal cardiac injury, as indicated by little to

no IgG^+ cardiac myocytes and negligible levels of serum cTnI that are not different from those observed in wild type mice. Corroborating the histological evidence of cardiomyocyte breakdown, serum levels of cTnI were found to be dramatically increased 8 hours after Iso administration in both mdx and C10 hearts. Serum collected from mdx mice 8 hours after the induction of Iso-induced injury showed 2.2-fold greater cTnI concentration than wild type mouse serum (Fig. 2C), consistent with the greater acute myocardial injury present in dystrophic hearts (Fig. 1B).

3.3. Fibrotic replacement of Iso-induced cardiac injury is dynamic.

Many, if not all, of the acutely damaged cardiomyocytes were removed following injury, resulting in their replacement with fibrotic lesions by 1 week after Iso administration. At timepoints of 1 week and 1 month following Iso-induced injury, dystrophic hearts displayed over 2-fold larger fibrosis area relative to wild type hearts (Fig. 3A), consistent with the elevated acute injury observed in mdx hearts at earlier timepoints. Replacement fibrosis area was highest 1 week following Iso administration in hearts from both strains, and closely reflected the peak acute injury area measured at 30 hours (Fig. 1B). Interestingly, 1 month after Iso-induced injury, total fibrotic lesion area was lower relative to its peak at 1 week after injury (Fig. 3A).

This curious observation of fibrotic area reduction between 1 week and 1 month following Iso administration could be explained by lesion contraction over this time period rather than by removal of deposited matrix. Collagen bundles display birefringence, the optical property that causes transmitted light to become polarized [53]. Collagen's orderly triple-helical structure underlies its inherent birefringence, which becomes more pronounced as the density of collagen fibers increases. Sirius Red staining further enhances this property due to the alignment of the dye molecule along the collagen strands [53–55]. Birefringence can be assessed microscopically by using two orthogonally-oriented polarized filters, referred to as the polarizer and the analyzer, flanking the sample [20]. Polarized light passing through the first filter (polarizer) and non-birefringent material will be blocked by the second filter (analyzer). However, a birefringent material will polarize the light further as it traverses, allowing some of it to pass through the analyzer and be detected by the camera. The wavelength and intensity of the light passing through the analyzer can provide information about the relative amount and organization of the birefringent material in the sample. For example, a diffuse patch of collagen fibers that are oriented in many directions results in a small amount of green or yellow polarized light. In contrast, a patch of densely-bundled and organized collagen strands would result in bright orange or red light, with structural collagen (e.g. tendons) serving as an excellent example of the latter [54–57]. Upon measuring the polarized light passing through prominent lesions of 1-week and 1-month mdx hearts, the older lesions were found to display a significantly greater birefringent area relative to the total area stained by Sirius Red (Fig. 3C). Accordingly, representative images show that the polarized light exiting 1-month-old lesions appears noticeably brighter with prominent areas of red and orange color (Fig. 3D), supporting the notion that tighter bundling of collagen over time is likely responsible for the modestly reduced area seen in older lesions.

3.4. Iso-induced injury triggers extensive immune cell infiltration in dystrophic hearts.

Infiltrating immune cells were labeled by antibody staining for CD45, a cell marker expressed by all leukocytes [58,59], and CD68, a phagocytic marker that is generally utilized as a differentiated macrophage marker [31,60–62]. Both of these immune cell markers showed a robust response to Iso-induced damage in mdx hearts, but this response was significantly attenuated and truncated in C10 hearts (Fig. 4A and 4D). Immune cell infiltration appeared to be delayed relative to the appearance of cardiac injury, with no response evident at 8 hours after Iso administration. In dystrophic hearts, an upsurge in immune infiltration could first be noted at 30 hours, with similarly robust immune cell presence lingering for at least 1 week following injury. In wild type hearts, a smaller increase in immune cells was apparent at 30 hours, and began to regress toward baseline levels 1 week post-injury. The prevalence of these immune cell markers dropped off to near-baseline levels 1 month post-injury in hearts from both strains.

In addition to different amplitudes of the peak response, immune infiltration also displayed different distribution in mdx and wild type hearts. $CD45^+$ leukocytes and $CD68^+$ macrophages were diffusely scattered throughout all of the hearts at baseline, and remained so up to 8 hours after injury. In dystrophic hearts, 30 hours and 1 week after injury both immune cell markers displayed robust expansion predominantly in regions of damage, evidenced by the majority of the cells clustering in lesion areas (Fig. 4B and 4E). Although wild type hearts showed significant immune expansion in lesion areas at the 30-hour timepoint, some augmentation of non-lesion immune cells was also observed. At least 50% or more of the immune cells continued to occupy non-lesion areas of wild type hearts at all timepoints, possibly due to the more diffuse nature of C10 cardiac injury.

3.5. Acute AT_1R blockade dramatically reduces dystrophic Iso-induced injury and modulates the immune response in the heart.

Angiotensin II (AngII) type 1 receptor (AT_1R) is expressed in many cell types, serving as a major mediator of AngII effects, including pro-fibrotic gene program activation and increased ROS production [63–67] (Fig. 5A). These outcomes can be attenuated by blocking activation of AT_1R with an angiotensin receptor blocker (ARB) like losartan. The anti-remodeling effects of ARBs are well-documented in long-term studies [12,68,69], but much less is known about the potential acute benefits of AT_1R blockade for the dystrophic heart. To shed more light on this question, mdx and wild type mice were treated with a brief course of intraperitoneal injections of losartan starting 1 hour before the bolus of Iso and spanning the period of 30 hours after Iso (Fig. 5A). Acute losartan treatment dramatically protected dystrophic hearts from cardiac damage following Iso injection, cutting mdx IgG^+ injury area by 2.8-fold (Fig. 5B). Conversely, AT_1R blockade showed no significant effect on wild type cardiac damage, resulting in comparable Iso-induced injury area in wild type and dystrophic hearts with acute losartan treatment. Interestingly, losartan did not change the distribution of lesions in dystrophic hearts, with mdx lesions remaining larger and localized more epicardially than C10 lesions (Fig. 5C).

The $CD45^+$ leukocyte response in 30-hour post-Iso hearts reflected the same trends as acute injury area. While C10 hearts showed no significant reduction in $CD45^+$ area with losartan,

mdx hearts showed a 38% reduction in the prevalence of CD45 after losartan treatment, resulting in CD45 levels that are not different from those observed in wild type hearts (Fig. 5D). Interestingly, $CD68^+$ macrophages showed a different trend, with a significant 53% reduction in total $CD68^+$ area in C10 hearts treated with losartan, despite no change in total injury area or total leukocyte infiltration (Fig. 5E). Dystrophic hearts also showed a trend toward a proportionately larger CD68 decline with losartan, with 56% lower CD68 compared to only 38% reduction in CD45. These declines in $CD68^+$ area appeared to manifest in both lesion and non-lesion areas in hearts of both strains, suggesting that the overall immune profile of these mice may have shifted as a consequence of AT_1R blockade (Fig. 5E). Representative images, highlighting lesion-positive areas in hearts of both strains, demonstrate the visibly reduced prominence of $CD68^+$ cellular infiltrates in losartan-treated groups (Fig. 5F).

4. DISCUSSION

Dystrophic cardiomyopathy is a progressive disorder in which the accumulation of lesions results in extensive fibrosis and global cardiac dysfunction. One major goal of the present study is to characterize myocardial injury in the dystrophic heart and the response to this injury over time. The cardiac injury protocol detailed here, resulting in a scattered distribution of myocardial lesions sustained secondary to increased workload on the heart, represents a physiologically relevant approach for modeling the injury that a dystrophic patient's heart might sustain during surgical procedures or other severely stressful events. This applicability is underscored by reports of elevated cardiac troponin I in DMD and Becker muscular dystrophy (BMD) patient serum [49,50], aligning with our observation of elevated cTnI in the serum of mdx mice following Iso-induced cardiac damage. Isoproterenol's well-characterized actions, ease of handling, and specificity for β-adrenergic receptors result in a simple and reproducible adrenergic stress model that can provide a reliable basis for evaluation of cardiac therapies. In addition to its utility in evaluating acute injury prevention as demonstrated here, this Iso-based injury model also provides quantifiable readouts for therapies that may target fibrosis or immune infiltration, broadening its applicability.

Another major goal of this work is to investigate whether intervention with angiotensin receptor blockers (ARBs) at the time of injury may help limit myocardial damage during the early necrotic phase, rather than only mitigating the cardiac remodeling during the later fibrotic period. ARBs may exert their action through multiple mechanisms downstream of angiotensin II type 1 receptor (AT_1R), a G-protein coupled receptor (GPCR) found widely expressed in many tissues, including cardiomyocytes and non-myocyte cardiac cells [70]. One pathway classically linked to AT_1R activation in the heart is the upregulation of genes associated with adverse remodeling, most notably TGF-β [64,71,72], a cytokine known to worsen dystrophic processes [73,74]. The inhibition of this pro-fibrotic and pro-hypertrophic gene program is often discussed as the main benefit of ARBs as a cardiac therapy. However, mounting evidence suggests that more acute effects of AT_1R activation include increased production of reactive oxygen species (ROS) by NADPH oxidase, a key mediator of angiotensin II's effects in many tissues [65,67]. Current literature features multiple reports of excessive NADPH oxidase-mediated superoxide production contributing to cardiac and

skeletal muscle injury in *mdx* mice [31,75–78], indicating that early treatment with ARBs is a promising approach for limiting dystrophic injury. Here we show that Iso-induced cardiac injury can be reduced 3-fold in dystrophic hearts by acute losartan treatment initiated 1 hour prior to adrenergic stress and maintained during the 30-hour period that followed it. This rapid protective effect strongly implicates an immediate signaling-based mechanism of action rather than transcriptional effects. Importantly, Iso-induced cardiac injury in wild type mice did not reflect any losartan benefit, suggesting that the mechanism of myocardial injury targeted by losartan's actions is uniquely exaggerated in dystrophic hearts. This notion is further supported by the different distributions of cardiac lesions in dystrophic and wild type hearts, even in the context of a strong reduction in dystrophic injury area. Wild type hearts display a peppering of small lesions clustered in endocardial regions, while mdx hearts show larger patches of damaged myocardium, which seem distributed at random throughout the walls of the heart. These mdx lesions become smaller and less frequent in losartan-treated hearts, but the distribution remains constant.

Our results, along with existing literature, support a model wherein ROS-mediated exacerbation of initial myocyte injury is a key driver of the accumulation of dystrophic heart damage. Oxidative stress induces a wide variety of pathological processes in the cell, including sarcolemmal damage, and has been thoroughly implicated in worsening cell survival [75,79]. NADPH oxidase, an effector of AT_1R signaling and an important source of reactive oxygen species within the heart, has been shown to have increased expression and activity in dystrophic muscle, and can be further activated in a stretch-dependent manner [80,81]. The approaches of specific inhibition of NADPH oxidase or general scavenging of ROS via N-acetylcysteine have been shown to improve both the skeletal muscle and cardiac phenotypes in dystrophic mice [31,75,76,78,82]. Together, these data suggest that AT_1R inhibition may benefit DMD patients by limiting the amplification of myocardial injury secondary to excessive ROS production in the dystrophic heart.

This work raises important questions regarding the mechanism of losartan action. The first question regards the significance of the altered immune response to cardiac injury, represented by the change in relative prevalence of macrophages. Wild type hearts showed a 53% reduction in $CD68^+$ area with losartan treatment, despite showing no significant changes in acute injury area or total $CD45^+$ leukocyte infiltration. A similar trend in relative proportions of immune cell markers can be observed in mdx hearts, where losartan treatment resulted in a 38% reduction in $CD45^+$ leukocytes, but a larger 56% reduction in $CD68^+$ cells. CD68 is a surface marker that is expressed to some degree by nearly all differentiated macrophages [61,62]. Similar reductions in CD68 content have been demonstrated in models of atherosclerosis and diabetic nephropathy treated with losartan [83,84]. Furthermore, it has been shown that macrophage AT_1R activation plays an important role in macrophage polarization toward the more pro-inflammatory M1 form and increased ROS production via macrophage NADPH oxidase [79,85,86]. If the immune response to cardiac damage is modified by losartan to become less inflammatory, then it's possible that both dystrophic and healthy hearts could derive delayed benefits from losartan in the form of more effective post-injury healing and less adverse remodeling.

Another important question is the relative benefit of ARB therapy compared to the broadly acting ACE inhibitors, which are currently more often prescribed to treat DMD patients despite showing lower tolerability [35,68]. Despite targeting similar physiological pathways, these two approaches have divergent effects on endogenous angiotensin signaling. ACE is a critical step in the enzymatic process that convert angiotensin I (AngI) to a variety of biologically active angiotensin peptides, including angiotensin II (AngII) and angiotensin (1-7). AngII may bind to both AT_1R and AT_2R, while angiotensin (1-7) binds to Mas receptor (MasR), triggering physiologically distinct downstream responses [87–89]. Importantly, signaling through AT_2R and MasR is considered to be protective, and is often characterized in terms of opposing the adverse pro-fibrotic and pro-inflammatory effects of AT_1R. ACE inhibition results in a large pool of uncleaved AngI, which, through the actions of non-ACE peptidases, may partially spill over into greater production of angiotensin (1-7) and greater MasR activation [90]. On the other hand, AT_1R blockade may leave large pools of both AngII and AngI [91], with much of the AngII presumably being displaced to signal more through AT_2R when AT_1R is inaccessible. Furthermore, ACE inhibition has been shown to alter the availability of bradykinin, another peptide associated with cardiac protection, by blocking its breakdown to inactive metabolites, whereas ARBs leave it unaffected [92,93]. Despite these differences, little work has been done to directly compare these two treatment approaches, and clinical trials in dystrophic patients have demonstrate that ARBs or ACEi have similar effects on the preservation of cardiac function when initiated after the onset of cardiac pathology [32]. Preclinical work has made only limited contributions to shedding light on this matter. Previous work using a 6-month or 2-year course of oral losartan demonstrated reductions in muscle fibrosis and cardiac remodeling, significantly preserved cardiac function, and markedly improved survival in losartan-treated mdx mice [94,95]. Comparable treatment courses with ACEi have not been documented in dystrophic mice. Studies using young, unstressed dystrophic mice with treatment periods of 2-4 months show mixed results, with most studies demonstrating little to no cardiac benefit compared to the natural disease course [96–98]. The short duration, lack of challenge, and co-administration of other drugs complicate the interpretation of the benefit of ACEi in dystrophic mice. The robust prevention of cardiac injury by AT_1R blockade presented here suggests that additional preclinical studies and patient trials should investigate the relative efficacy of ARB-based versus ACEi-based therapeutic approaches in limiting cardiac dysfunction when initiated prior to clinically evident cardiac disease.

Current best practice recommendations suggest that anti-angiotensin therapy should be initiated in DMD patients by the age of 10 [2,3]. This recommendation is based on a trial of the ACEi perindopril, in which the group of patients that initiated therapy at 10.7 ± 1.2 years of age demonstrated better cardiac function 5 years later and higher 10-year survival than the group that started therapy at 13.6 ± 1.2 years of age [99,100]. This clinical trial underscores the importance of early initiation of therapy. However, the observation that global cardiac dysfunction can be detected in patients at the age of 10 indicates that the loss of myocardium likely begins much earlier [1,39]. A significant concern with early initiation of cardiac therapy in the pediatric patient population is that potential side effects may significantly impact quality of life. The issue of tolerability has been studied in over 250,000 heart failure patients, demonstrating that ACEi and ARBs are equally effective, but ARBs are

significantly better tolerated [101,102]. The new discovery of a striking benefit for acute myocardial injury shown here, coupled with limited side effects, strongly supports inclusion of ARBs among the first interventions to limit cardiomyopathy in DMD patients, well before the onset of global cardiac dysfunction. The earliest age at which any cardiac damage can be identified remains unclear, but it is clear that once myocardial damage occurs, it is lost forever.

The studies presented here provide a new, readily reproducible model of inducing cardiac injury in a genetic model of DMD. This approach provides an excellent platform for the study of myocardial injury responses, and offers significant potential for the pre-clinical assessment of therapies directed at dystrophic cardiomyopathy. The nature of the progression of dystrophic cardiomyopathy is unclear, but recent evidence suggests that DMD patients experience periods of significant cardiac damage resulting in elevations in serum markers of cardiac injury [1,39–41]. These episodic periods of cardiac injury are closely mirrored by the Iso-induced injury model used in these studies. The heart disease associated with DMD is of growing clinical importance, however many of the new therapeutic approaches have limited efficacy in the heart. Using this new model system, we demonstrate the acute protective capability of losartan pre-treatment in limiting the extent of new cardiac injury. This raises the important possibility that AT_1R blockade may not only result in favorable cardiac remodeling, but may limit the accumulation of injury in the first place. If true, early ARB therapy could significantly delay the onset of cardiac dysfunction in DMD patients, extending survival and improving their quality of life.

ACKNOWLEDGMENTS

The β-adrenergic receptor knockout mice were provided by Dr. B.B. Lowell, Beth Israel Deaconess Medical Center. The authors thank Dr. Anthony Vetter (University of Minnesota) for assistance with preparation of the manuscript.

This work was supported by the National Institutes of Health (R01 HL114832 and K08HL102066 to DT, F31HL139093 to TAM), the Muscular Dystrophy Association (Grant 351960 to DT), stipends from the Lillehei Heart Institute and the Greg Marzolf Jr. Foundation to AK, and the University of Minnesota.

Abbreviations:

DMD	Duchenne muscular dystrophy
AT_1R	angiotensin II type 1 receptor
Iso	isoproterenol
ACEi	angiotensin converting enzyme inhibitor
ARB	angiotensin receptor blocker
cTnI	cardiac troponin I
cTnT	cardiac troponin T
AngII	angiotensin II
AngI	angiotensin I

WGA	wheat germ agglutinin
MasR	Mas receptor
AT_2R	angiotensin II type 2 receptor
ROS	reactive oxygen species

REFERENCES

[1]. Nigro G, Comi LI, Politano L, Bain RJ, The incidence and evolution of cardiomyopathy in Duchenne muscular dystrophy, Int J Cardiol. 26 (1990) 271–277. [PubMed: 2312196]

[2]. Birnkrant DJ, Bushby K, Bann CM, Alman BA, Apkon SD, Blackwell A, Case LE, Cripe L, Hadjiyannakis S, Olson AK, Sheehan DW, Bolen J, Weber DR, Ward LM, Diagnosis and management of Duchenne muscular dystrophy, part 2: respiratory, cardiac, bone health, and orthopaedic management, Lancet Neurol. 17 (2018) 347–361. doi:10.1016/S1474-4422(18)30025-5. [PubMed: 29395990]

[3]. McNally EM, Kaltman JR, Benson DW, Canter CE, Cripe LH, Duan D, Finder JD, Groh WJ, Hoffman EP, Judge DP, Kertesz N, Kinnett K, Kirsch R, Metzger JM, Pearson GD, Rafael-Fortney JA, Raman SV, Spurney CF, Targum SL, Wagner KR, Markham LW, and B I. Working Group of the National Heart, Lung, Parent Project Muscular Dystrophy, Contemporary cardiac issues in duchenne muscular dystrophy., Circulation. 131 (2015) 1590–8. doi:10.1161/CIRCULATIONAHA.114.015151. [PubMed: 25940966]

[4]. Spurney CF, Cardiomyopathy of Duchenne muscular dystrophy: current understanding and future directions, Muscle Nerve. 44 (2011) 8–19. doi:10.1002/mus.22097. [PubMed: 21674516]

[5]. Muntoni F, Cardiomyopathy in muscular dystrophies, Curr. Opin. Neurol 16 (2003) 577–583. doi:10.1097/00019052-200310000-00003. [PubMed: 14501841]

[6]. Mah JK, Korngut L, Dykeman J, Day L, Pringsheim T, Jette N, A systematic review and meta-analysis on the epidemiology of Duchenne and Becker muscular dystrophy, Neuromuscul. Disord 24 (2014) 482–491. doi:10.1016/j.nmd.2014.03.008. [PubMed: 24780148]

[7]. Hoffman EP, Brown RH, Kunkel LM, Dystrophin: the protein product of the Duchene muscular dystrophy locus, Cell. 51 (1987) 919–928. [PubMed: 3319190]

[8]. Hoffman EP, Kunkel LM, Dystrophin abnormalities in Duchenne/Becker muscular dystrophy, Neuron. 2(1989) 1019–1029. doi:10.1016/0896-6273(89)90226-2. [PubMed: 2696500]

[9]. Campbell KP, Ervasti JM, Dystrophin and the membrane skeleton, Curr. Opin. Cell Biol 5 (1993) 82–87. doi:10.1016/S0955-0674(05)80012-2. [PubMed: 8448034]

[10]. Allen DG, Whitehead NP, Duchenne muscular dystrophy - What causes the increased membrane permeability in skeletal muscle?, Int. J. Biochem. Cell Biol 43 (2010) 290–294. doi:10.1016/j.biocel.2010.11.005. [PubMed: 21084059]

[11]. Ervasti JM, Sonnemann KJ, Biology of the Striated Muscle Dystrophin-Glycoprotein Complex, Int. Rev. Cytol 265 (2008) 191–225. doi:10.1016/S0074-7696(07)65005-0. [PubMed: 18275889]

[12]. Wagner KR, Approaching a New Age in Duchenne Muscular Dystrophy Treatment, Neurotherapeutics. 5(2008) 583–591. [PubMed: 19019310]

[13]. Chamberlain JS, Metzger J, Reyes M, Townsend D, Faulkner JA, Dystrophin-deficient mdx mice display a reduced life span and are susceptible to spontaneous rhabdomyosarcoma, FASEB J. 21 (2007) 2195–2204. http://www.ncbi.nlm.nih.gov/pubmed/17360850. [PubMed: 17360850]

[14]. Birnkrant DJ, Bushby K, Bann CM, Apkon SD, Blackwell A, Brumbaugh D, Case LE, Clemens PR, Hadjiyannakis S, Pandya S, Street N, Tomezsko J, Wagner KR, Ward LM, Weber DR, Diagnosis and management of Duchenne muscular dystrophy, part 1: diagnosis, and neuromuscular, rehabilitation, endocrine, and gastrointestinal and nutritional management, Lancet Neurol. 17 (2018) 211–212. doi:10.1016/S1474-4422(18)30024-3.

[15]. Eagle M, Baudouin SV, Chandler C, Giddings DR, Bullock R, Bushby K, Survival in Duchenne muscular dystrophy: improvements in life expectancy since 1967 and the impact of home

nocturnal ventilation, Neuromuscul. Disord 12 (2002)926–929. doi:10.1016/S0960-8966(02)00140-2. [PubMed: 12467747]

[16]. Rafael-Fortney JA, Chadwick JA, Raman SV, Duchenne Muscular Dystrophy Mice and Men: Can Understanding a Genetic Cardiomyopathy Inform Treatment of Other Myocardial Diseases?, Circ. Res 118 (2016) 1059–1061. doi:10.1161/CIRCRESAHA.116.308402. [PubMed: 27034274]

[17]. Bulfield G, Siller WG, Wight PA, Moore KJ, X chromosome-linked muscular dystrophy (mdx) in the mouse, Proc Natl Acad Sci U S A. 81 (1984) 1189–1192. http://www.ncbi.nlm.nih.gov/pubmed/6583703. [PubMed: 6583703]

[18]. Ryder-Cook AS, Sicinski P, Thomas K, Davies KE, Worton RG, Barnard EA, Darlison MG, Barnard PJ, Localization of the mdx mutation within the mouse dystrophin gene., EMBO J. 7 (1988) 3017–3021. [PubMed: 2903046]

[19]. McGreevy JW, Hakim CH, McIntosh MA, Duan D, Animal models of Duchenne muscular dystrophy: from basic mechanisms to gene therapy, Dis. Model. Mech 8 (2015) 195–213. doi:10.1242/dmm.018424. [PubMed: 25740330]

[20]. Meyers TA, Townsend D, Early right ventricular fibrosis and reduction in biventricular cardiac reserve in the dystrophin-deficient mdx heart, Am. J. Physiol. - Hear. Circ. Physiol 308 (2015) H303–H315. doi:10.1152/ajpheart.00485.2014.

[21]. Spurney CF, Guerron AD, Yu Q, Sali A, van der Meulen JH, Hoffman EP, Nagaraju K, Membrane sealant Poloxamer P188 protects against isoproterenol induced cardiomyopathy in dystrophin deficient mice., BMC Cardiovasc. Disord 11 (2011) 20. doi:10.1186/1471-2261-11-20. [PubMed: 21575230]

[22]. Rafael-Fortney JA, Chimanji NS, Schill KE, Martin CD, Murray JD, Ganguly R, Stangland JE, Tran T, Xu Y, Canan BD, Mays TA, Delfín DA, Janssen PML, Raman SV, Early treatment with lisinopril and spironolactone preserves cardiac and skeletal muscle in Duchenne muscular dystrophy mice, Circulation. 124 (2011) 582–588. doi:10.1161/CIRCULATIONAHA.111.031716. [PubMed: 21768542]

[23]. Yue Y, Skimming JW, Liu M, Strawn T, Duan D, Full-length dystrophin expression in half of the heart cells ameliorates β-isoproterenol-induced cardiomyopathy in mdx mice, Hum. Mol. Genet 13 (2004) 1669–1675. doi:10.1093/hmg/ddh174. [PubMed: 15190010]

[24]. Townsend D, Blankinship MJ, Allen JM, Gregorevic P, Chamberlain JS, Metzger JM, Systemic administration of micro-dystrophin restores cardiac geometry and prevents dobutamine-induced cardiac pump failure, Mol Ther. 15 (2007) 1086–1092. http://www.ncbi.nlm.nih.gov/pubmed/17440445. [PubMed: 17440445]

[25]. Townsend D, Yasuda S, McNally E, Metzger JM, Distinct pathophysiological mechanisms of cardiomyopathy in hearts lacking dystrophin or the sarcoglycan complex, FASEB J. 25 (2011) 3106–3114. doi:10.1096/fj.10-178913. [PubMed: 21665956]

[26]. Heydemann, Ceco E, Lim JE, Hadhazy M, Ryder P, Moran JL, Beier DR, Palmer AA, McNally EM, Latent TGF-β - binding protein 4 modifies muscular dystrophy in mice, 119 (2009). doi:10.1172/JCI39845.Phenotypic.

[27]. Lorts, Schwanekamp JA, Baudino TA, McNally EM, Molkentin JD, Deletion of periostin reduces muscular dystrophy and fibrosis in mice by modulating the transforming growth factor-β pathway., Proc. Natl. Acad. Sci. U. S. A 109 (2012) 10978–83. doi:10.1073/pnas.1204708109. [PubMed: 22711826]

[28]. Cohn RD, Van Erp C, Habashi JP, Soleimani AA, Klein EC, Lisi MT, Gamradt M, Rhys CM, Holm TM, Loeys BL, Ramirez F, Judge DP, Ward CW, Dietz HC, Angiotensin II type 1 receptor blockade attenuates TGF- b – induced failure of muscle regeneration in multiple myopathic states, 13 (2007) 204–211. doi:10.1038/nm1536.

[29]. Tidball JG, Wehling-Henricks M, The role of free radicals in the pathophysiology of muscular dystrophy, J. Appl. Physiol 102 (2007) 1677–1686. doi:10.1152/japplphysiol.01145.2006. [PubMed: 17095633]

[30]. Chadwick JA, Swager SA, Lowe J, Welc SS, Tidball JG, Gomez-Sanchez CE, Gomez-Sanchez EP, Rafael-Fortney JA, Myeloid cells are capable of synthesizing aldosterone to exacerbate damage in muscular dystrophy, Hum. Mol. Genet 25(2016) 5167–5177. doi:10.1093/hmg/ddw331. [PubMed: 27798095]

[31]. Williams IA, Allen DG, The role of reactive oxygen species in the hearts of dystrophin-deficient mdx mice, Am. J. Physiol. - Hear. Circ. Physiol 293 (2007) H1969–H1977. doi:10.1152/ajpheart.00489.2007.

[32]. Allen HD, Flanigan KM, Thrush PT, Viollet-Callendret L, Dvorchik I, Yin H, Canter CE, Connolly AM, Parrish M, McDonald CM, Braunlin E, Colan SD, Day J, Darras B, Mendell JR, Randomized A, Double-Blind Trial of Lisinopril and Losartan for the Treatment of Cardiomyopathy in Duchenne Muscular Dystrophy, PLoS Curr. Muscular Dystrophy. 1 (2013). doi:10.1371/currents.md.2cc69a1dae4be7dfe2bcb420024ea865.

[33]. Viollet L, Thrush PT, Flanigan KM, Mendell JR, Allen HD, Effects of angiotensin-converting enzyme inhibitors and/or beta blockers on the cardiomyopathy in Duchenne muscular dystrophy, Am. J. Cardiol 110(2012) 98–102. doi:10.1016/j.amjcard.2012.02.064. [PubMed: 22463839]

[34]. Whitehead NP, Pham C, Gervasio OL, Allen DG, N-Acetylcysteine ameliorates skeletal muscle pathophysiology in mdx mice, J. Physiol 586 (2008) 2003–2014. doi:10.1113/jphysiol.2007.148338. [PubMed: 18258657]

[35]. Russo V, Papa AA, Williams EA, Rago A, Palladino A, Politano L, Nigro G, ACE inhibition to slow progression of myocardial fibrosis in muscular dystrophies, Trends Cardiovasc. Med 28 (2018) 330–337. doi:10.1016/j.tcm.2017.12.006. [PubMed: 29292032]

[36]. Pinto R. de Senzi Moraes, Ferretti R, Moraes LHR, Neto HS, Marques MJ, Minatel E, N-Acetylcysteine treatment reduces TNF-α levels and myonecrosis in diaphragm muscle of mdx mice, Clin. Nutr 32 (2013) 472–475. doi:10.1016/j.clnu.2012.06.001. [PubMed: 22727548]

[37]. Lee E-M, Kim D-Y, Kim A-Y, Lee E-J, Kim S-H, Lee M-M, Sung S-E, Park J-K, Jeong K-S, Chronic effects of losartan on the muscles and the serologic profiles of mdx mice, Life Sci. 143 (2015) 35–42. doi:10.1016/j.lfs.2015.10.023. [PubMed: 26497927]

[38]. Guiraud S, Davies KE, Pharmacological advances for treatment in Duchenne muscular dystrophy, Curr. Opin. Pharmacol 34 (2017) 36–48. doi:10.1016/j.coph.2017.04.002. [PubMed: 28486179]

[39]. Markham LW, Michelfelder EC, Border WL, Khoury PR, Spicer RL, Wong BL, Benson DW, Cripe LH, Abnormalities of Diastolic Function Precede Dilated Cardiomyopathy Associated with Duchenne Muscular Dystrophy, J. Am. Soc. Echocardiogr 19 (2006) 865–871. doi:10.1016/j.echo.2006.02.003. [PubMed: 16824995]

[40]. McNally EM, New Approaches in the Therapy of Cardiomyopathy in Muscular Dystrophy, Annu. Rev. Med 58 (2007) 75–88. doi:10.1146/annurev.med.58.011706.144703. [PubMed: 17217326]

[41]. Kirchmann, Kececioglu D, Korinthenberg R, Dittrich S, Echocardiographic and electrocardiographic findings of cardiomyopathy in Duchenne and Becker-Kiener muscular dystrophies, Pediatr Cardiol. 26 (2005) 66–72. [PubMed: 15793655]

[42]. Strakova J, Dean JD, Sharpe K, Meyers TA, Odom G, Townsend D, Dystrobrevin increases dystrophin's binding to the dystrophin-glycoprotein complex and provides protection during cardiac stress., J. Mol. Cell. Cardiol 76(2014) 106–115. doi:10.1016/j.yjmcc.2014.08.013. [PubMed: 25158611]

[43]. Yasuda S, Townsend D, Michele DE, Favre EG, Day SM, Metzger JM, Dystrophic heart failure blocked by membrane sealant poloxamer, Nature. 436 (2005) 1025–1029. http://www.ncbi.nlm.nih.gov/pubmed/16025101. [PubMed: 16025101]

[44]. Tuttle RR, Mills J, Dobutamine: Development of a new catecholamine to selectively increase cardiac contractility, Circ. Res 36 (1975) 185–196. doi:10.1161/01.RES.36.1.185. [PubMed: 234805]

[45]. Schmidt GN, Burmeister MA, Lilje C, Wappler F, Bischoff P, Acute heart failure during spinal surgery in a boy with Duchenne muscular dystrophy, Br J Anaesth. 90 (2003) 800–804. [PubMed: 12765898]

[46]. Tamaki T, Nishiyama A, Kimura S, Aki Y, Yoshizumi M, Houchi H, Morita K, Abe Y, EXP3174: The Major Active Metabolite of Losartan, Cardiovasc. Drug Rev 15 (1997) 122–136. doi:10.1111/j.1527-3466.1997.tb00327.x.

[47]. Lo MW, Goldberg MR, McCrea JB, Lu H, Furtek CI, Bjornsson TD, Pharmacokinetics of losartan, an angiotensin II receptor antagonist, and its active metabolite EXP3174 in humans,

Clin. Pharmacol. Ther 58 (1995) 641–649. doi:10.1016/0009-9236(95)90020-9. [PubMed: 8529329]

[48]. R.C. Team, R: A language and environment for statistical computing., (2017) http://www.r-project.org/. http://www.r-project.org/.

[49]. Hor KN, Johnston P, Kinnett K, Mah ML, Stiver C, Markham L, Cripe L, Progression of Duchenne Cardiomyopathy Presenting with Chest Pain and Troponin Elevation., J. Neuromuscul. Dis 4 (2017) 307–314. doi:10.3233/JND-170253. [PubMed: 28984614]

[50]. Matsumura T, Saito T, Fujimura H, Shinno S, Cardiac troponin I for accurate evaluation of cardiac status in myopathic patients, Brain Dev. 29 (2007) 496–501. doi:10.1016/j.braindev.2007.01.009. [PubMed: 17376624]

[51]. Ergul Y, Ekici B, Nisli K, Tatli B, Binboga F, Acar G, Ozmen M, Omeroglu RE, Evaluation of the North Star Ambulatory Assessment scale and cardiac abnormalities in ambulant boys with Duchenne muscular dystrophy., J. Paediatr. Child Health 48 (2012) 610–6. doi:10.1111/j.1440-1754.2012.02428.x. [PubMed: 22404693]

[52]. Ramaciotti, lannaccone ST, Scott WA, Myocardial cell damage in Duchenne muscular dystrophy, Pediatr Cardiol. 24 (2003) 503–506. doi:10.1007/s00246-002-0408-9. [PubMed: 14627325]

[53]. Junqueira LC, Bignolas G, Brentani RR, Picrosirius staining plus polarization microscopy, a specific method for collagen detection in tissue sections., Histochem. J 11 (1979)447–55. http://www.ncbi.nlm.nih.gov/pubmed/91593. [PubMed: 91593]

[54]. Lattouf R, Younes R, Lutomski D, Naaman N, Godeau G, Senni K, Changotade S, Picrosirius Red Staining: A Useful Tool to Appraise Collagen Networks in Normal and Pathological Tissues, J. Histochem. Cytochem 62 (2014) 751–758. doi:10.1369/0022155414545787. [PubMed: 25023614]

[55]. Rich L, Whittaker P, Collagen and Picrosirius red staining: a polarized light assessment of fibrillar hue and spatial distribution, Brazilian J. Morphol. Sci 22 (2005) 97–104. doi:10.1016/j.eurpolymj.2004.01.020.

[56]. Junqueira LC, Montes GS, Sanchez EM, The influence of tissue section thickness on the study of collagen by the Picrosirius-polarization method., Histochemistry. 74 (1982) 153–6. http://www.ncbi.nlm.nih.gov/pubmed/7085347. [PubMed: 7085347]

[57]. Dayan, Hirshberg A, Woiman M.Aviv T, Hiss Y, Bubis JJ, Wolman M, Are the polarization colors of picrosirius red-stained collagen determined only by the diameter of the fibers?, Histochemistry. 93 (1989) 27–9. http://www.ncbi.nlm.nih.gov/pubmed/2482274. [PubMed: 2482274]

[58]. Hermiston ML, Xu Z, Weiss A, CD45: A Critical Regulator of Signaling Thresholds in Immune Cells, Annu. Rev. Immunol 21 (2003) 107–37. doi:10.1146/annurev.immunol.21.120601.140946. [PubMed: 12414720]

[59]. Patties, Haagen J, Dörr W, Hildebrandt G, Glasow A, Late inflammatory and thrombotic changes in irradiated hearts of C57BL/6 wild-type and atherosclerosis-prone ApoE-deficient mice, Strahlentherapie Und Onkol. 191 (2015) 172–179. doi:10.1007/s00066-014-0745-7.

[60]. Barros MHM, Hauck F, Dreyer JH, Kempkes B.Niedobitek G, Macrophage polarisation: An immunohistochemical approach for identifying M1 and M2 macrophages, PLoS One. 8 (2013) 1–11. doi:10.1371/journal.pone.0080908.

[61]. Raggi, Pelassa S, Pierobon D, Penco F, Gattorno M, Novelli F, Eva A, Varesio L, Giovarelli M, Bosco MC, Regulation of human Macrophage M1-M2 Polarization Balance by hypoxia and the Triggering receptor expressed on Myeloid cells-1, Front. Immunol 8 (2017) 1097. doi:10.3389/fimmu.2017.01097. [PubMed: 28936211]

[62]. Genin M, Clement F, Fattaccioli A, Raes M, Michiels C, M1 and M2 macrophages derived from THP-1 cells differentially modulate the response of cancer cells to etoposide, BMC Cancer. 15 (2015) 577. doi:10.1186/s12885-015-1546-9. [PubMed: 26253167]

[63]. Kharraz Y, Guerra J, Pessina P, Serrano AL, Muñoz-Cánoves P, Understanding the Process of Fibrosis in Duchenne Muscular Dystrophy., Biomed Res. Int 2014 (2014) 965631. doi:10.1155/2014/965631. [PubMed: 24877152]

[64]. Rosenkranz S, TGF-β1 and angiotensin networking in cardiac remodeling, Cardiovasc. Res 63 (2004) 423–432. doi:10.1016/j.cardiores.2004.04.030. [PubMed: 15276467]

[65]. Dikalov SI, Nazarewicz RR, Angiotensin II-Induced Production of Mitochondrial Reactive Oxygen Species: Potential Mechanisms and Relevance for Cardiovascular Disease, Antioxid. Redox Signal. 19 (2013) 1085–1094. doi:10.1089/ars.2012.4604. [PubMed: 22443458]

[66]. Choi H, Leto TL, Hunyady L, Catt KJ, Yun SB, Sue GR, Mechanism of angiotensin II-induced superoxide production in cells reconstituted with angiotensin type 1 receptor and the components of NADPH oxidase, J. Biol. Chem 283 (2008) 255–267. doi:10.1074/jbc.M708000200. [PubMed: 17981802]

[67]. Münzel T, Gori T, Keaney JF, Maack C, Daiber A, Pathophysiological role of oxidative stress in systolic and diastolic heart failure and its therapeutic implications, Eur. Heart J 36 (2015) 2555–2564. doi:10.1093/eurheartj/ehv305. [PubMed: 26142467]

[68]. Munger MA, Use of Angiotensin receptor blockers in cardiovascular protection: Current evidence and future directions, Pharm. Ther 36 (2011) 22–40.

[69]. Sukumaran V, Watanabe K, Veeraveedu PT, Thandavarayan RA, Gurusamy N, Ma M, Yamaguchi K, Suzuki K, Kodama M, Aizawa Y, Telmisartan, an angiotensin-II receptor blocker ameliorates cardiac remodeling in rats with dilated cardiomyopathy, Hypertens. Res 33 (2010) 695–702. doi:10.1038/hr.2010.67. [PubMed: 20535115]

[70]. Dasgupta, Zhang L, Angiotensin II receptors and drug discovery in cardiovascular disease, Drug Discov. Today 16 (2011)22–34. doi:10.1016/j.drudis.2010.11.016. [PubMed: 21147255]

[71]. Khan R, Sheppard R, Fibrosis in heart disease: Understanding the role of transforming growth factor-β1 in cardiomyopathy, valvular disease and arrhythmia, Immunology. 118 (2006) 10–24. doi:10.1111/j.1365-2567.2006.02336.X. [PubMed: 16630019]

[72]. Porter KE, Turner NA, Cardiac fibroblasts: At the heart of myocardial remodeling, Pharmacol. Ther 123 (2009) 255–278. doi:10.1016/j.pharmthera.2009.05.002. [PubMed: 19460403]

[73]. Heydemann, Huber JM, Kakkar R, Wheeler MT, McNally EM, Functional nitric oxide synthase mislocalization in cardiomyopathy, J Mol Cell Cardiol. 36 (2004) 213–223. doi:10.1016/j.yjmcc.2003.09.020 S0022282803003031 [pii]. [PubMed: 14871549]

[74]. Flanigan KM, Ceco E, Lamar K-M, Kaminoh Y, Dunn DM, Mendell JR, King WM, Pestronk A, Florence JM, Mathews KD, Finkel RS, Swoboda KJ, Gappmaier E, Howard MT, Day JW, McDonald C, McNally EM, Weiss RB, LTBP4 genotype predicts age of ambulatory loss in duchenne muscular dystrophy., Ann. Neurol 73 (2013) 481–488. doi:10.1002/ana.23819. [PubMed: 23440719]

[75]. Allen DG, Whitehead NP, Froehner SC, Absence of Dystrophin Disrupts Skeletal Muscle Signaling: Roles of Ca2+, Reactive Oxygen Species, and Nitric Oxide in the Development of Muscular Dystrophy, Physiol. Rev 96 (2015) 253–305. doi:10.1152/physrev.00007.2015.

[76]. Gonzalez DR, Treuer AV, Lamirault G, Mayo V, Cao Y, Dulce RA, Hare JM, NADPH oxidase-2 inhibition restores contractility and intracellular calcium handling and reduces arrhythmogenicity in dystrophic cardiomyopathy, AJP Hear. Circ. Physiol 307 (2014) H710–H721. doi:10.1152/ajpheart.00890.2013.

[77]. Cozzoli, Liantonio A, Conte E, Cannone M, Massari AM, Giustino A, Scaramuzzi A, Pierno S, Mantuano P, Capogrosso RF, Camerino GM, De Luca A, Angiotensin II modulates mouse skeletal muscle resting conductance to chloride and potassium ions and calcium homeostasis via the AT1 receptor and NADPH oxidase, AJP Cell Physiol. 307 (2014) C634–C647. doi:10.1152/ajpcell.00372.2013.

[78]. Olthoff JT, Lindsay A, Abo-Zahrah R, Baltgalvis KA, Patrinostro X, Belanto JJ, Yu D-Y, Perrin BJ, Garry DJ, Rodney GG, Lowe DA, Ervasti JM, Loss of peroxiredoxin-2 exacerbates eccentric contraction-induced force loss in dystrophin-deficient muscle, Nat. Commun 9 (2018) 5104. doi:10.1038/s41467-018-07639-3. [PubMed: 30504831]

[79]. Bedard K, Krause K-H, The NOX family of ROS-generating NADPH oxidases: physiology and pathophysiology, Physiol. Rev 87 (2007) 245–313. doi:10.1152/physrev.00044.2005. [PubMed: 17237347]

[80]. Prosser BL, Ward CW, Lederer WJ, X-ROS Signaling: Rapid Mechano-Chemo Transduction in Heart, Science. 333 (2011) 1440–1446. doi:10.1126/science.1202768. [PubMed: 21903813]

[81]. Prosser BL, Khairallah RJ, Ziman AP, Ward CW, Lederer WJ, X-ROS signaling in the heart and skeletal muscle: Stretch-dependent local ROS regulates [Ca2+]i, J. Mol. Cell. Cardiol 58 (2013) 172–181. doi:10.1016/j.yjmcc.2012.11.011. [PubMed: 23220288]

[82]. Ismail HM, Scapozza L, Ruegg UT, Dorchies OM, Diapocynin, a Dimer of the NADPH Oxidase Inhibitor Apocynin, Reduces ROS Production and Prevents Force Loss in Eccentrically Contracting Dystrophic Muscle., PLoS One. 9 (2014) e110708. doi:10.1371/journal.pone.0110708. [PubMed: 25329652]

[83]. Yang J, Zhang X, Yu X, Tang W, Gan H, Renin-Angiotensin system activation accelerates atherosclerosis in experimental renal failure by promoting endoplasmic reticulum stress-related inflammation, Int. J. Mol. Med 39(2017) 613–621. doi:10.3892/ijmm.2017.2856. [PubMed: 28098884]

[84]. Yao Y, Li Y, Zeng X, Ye Z, Li X, Zhang L, Losartan Alleviates Renal Fibrosis and Inhibits Endothelial-to-Mesenchymal Transition (EMT) Under High-Fat Diet-Induced Hyperglycemia, Front. Pharmacol 9 (2018) 1213. doi:10.3389/fphar.2018.01213. [PubMed: 30420805]

[85]. Fujisaka S, Usui I, Kanatani Y, Ikutani M, Takasaki I, Tsuneyama K, Tabuchi Y, Bukhari A, Yamazaki Y, Suzuki H, Senda S, Aminuddin A, Nagai Y, Takatsu K, Kobayashi M, Tobe K, Telmisartan improves insulin resistance and modulates adipose tissue macrophage polarization in high-fat-fed mice, Endocrinology. 152 (2011) 1789–1799. doi:10.1210/en.2010-1312. [PubMed: 21427223]

[86]. Yamamoto S, Yancey PG, Zuo Y, Ma L-J, Kaseda R, Fogo AB, Ichikawa I, Linton MF, Fazio S, Kon V, Macrophage polarization by angiotensin II-type 1 receptor aggravates renal injury-acceleration of atherosclerosis, Arterioscler. Thromb. Vase. Biol 31 (2011) 2856–2864. doi:10.1161/ATVBAHA.111.237198.

[87]. Westermeier, Bustamante M, Pavez M, Garcia L, Chiong M, Ocaranza MP, Lavandero S, Novel players in cardioprotection: Insulin like growth factor-1, angiotensin-(1-7) and angiotensin-(1-9), Pharmacol. Res 101 (2015) 41–55. doi:10.1016/j.phrs.2015.06.018. [PubMed: 26238180]

[88]. Chappell MC, Marshall AC, Alzayadneh EM, Shaltout HA, Diz DI, Update on the angiotensin converting enzyme 2-angiotensin (1–7)-Mas receptor axis: fetal programing, sex differences, and intracellular pathways, Front. Endocrinol. (Lausanne). 4 (2014) 201. doi:10.3389/fendo.2013.00201. [PubMed: 24409169]

[89]. Santos RA, Angiotensin-(1-7), Hypertension. 63(2014) 1138–1147. doi:10.1161/HYPERTENSIONAHA.113.01274. [PubMed: 24664288]

[90]. Basu R, Poglitsch M, Yogasundaram H, Thomas J, Rowe BH, Oudit GY, Roles of Angiotensin Peptides and Recombinant Human ACE2 in Heart Failure, J. Am. Coll. Cardiol 69 (2017) 805–819. doi:10.1016/j.jacc.2016.11.064. [PubMed: 28209222]

[91]. Pavo N, Goliasch G, Wurm R, Novak J, Strunk G, Gyöngyösi M, Poglitsch M, Säemann MD, Hülsmann M, Low- and high-renin heart failure phenotypes with clinical implications, Clin. Chem 64 (2018) 597–608. doi:10.1373/clinchem.2017.278705. [PubMed: 29138270]

[92]. Manolis AJ, Marketou ME, Gavras I, Gavras H, Cardioprotective properties of bradykinin: role of the B2 receptor, Hypertens. Res 33 (2010) 772–777. doi:10.1038/hr.2010.82. [PubMed: 20505673]

[93]. Hartman JC, The role of bradykinin and nitric oxide in the cardioprotective action of ACE inhibitors, Ann. Thorac. Surg 60 (1995) 789–792. doi:10.1016/0003-4975(95)00192-N. [PubMed: 7545893]

[94]. Spurney CF, Sali A, Guerron AD, lantorno M, Yu Q, Gordish-Dressman H, Rayavarapu S, Van Der Meulen J, Hoffman EP, Nagaraju K, Losartan decreases cardiac muscle fibrosis and improves cardiac function in dystrophin-deficient mdx mice, J. Cardiovasc. Pharmacol. Ther 16 (2011) 87–95. doi:10.1177/1074248410381757. [PubMed: 21304057]

[95]. Bish LT, Yarchoan M, Sleeper MM, Gazzara JA, Morine KJ, Acosta P, Barton ER, Sweeney HL, Chronic Losartan Administration Reduces Mortality and Preserves Cardiac but Not Skeletal Muscle Function in Dystrophic Mice, PLoS One. 6 (2011) e20856. doi:10.1371/journal.pone.0020856. [PubMed: 21731628]

[96]. Bauer R, Straub V, Blain A, Bushby K, MacGowan GA, Contrasting effects of steroids and angiotensin-converting-enzyme inhibitors in a mouse model of dystrophin-deficient

cardiomyopathy, Eur. J. Heart Fail 11 (2009)463–471. doi:10.1093/eurjhf/hfp028. [PubMed: 19233868]

[97]. Blain, Greally E, Laval SH, Blamire AM, MacGowan G. a., Straub VW, Absence of Cardiac Benefit with Early Combination ACE Inhibitor and Beta Blocker Treatment in mdx Mice, J. Cardiovasc. Transl. Res 8 (2015) 198–207. doi:10.1007/s12265-015-9623-7. [PubMed: 25896492]

[98]. Janssen PML, Murray JD, Schill KE, Rastogi N, Schultz EJ, Tran T, Raman SV, Rafael-Fortney JA, Prednisolone Attenuates Improvement of Cardiac and Skeletal Contractile Function and Histopathology by Lisinopril and Spironolactone in the mdx Mouse Model of Duchenne Muscular Dystrophy., PLoS One. 9 (2014) e88360. doi:10.1371/journal.pone.0088360. [PubMed: 24551095]

[99]. Duboc, Meune C, Lerebours G, Devaux JY, Vaksmann G, Bécane HM, Effect of perindopril on the onset and progression of left ventricular dysfunction in Duchenne muscular dystrophy, J. Am. Coll. Cardiol 45 (2005) 855–857. doi:10.1016/j.jacc.2004.09.078. [PubMed: 15766818]

[100]. Duboc, Meune C, Pierre B, Wahbi K, Eymard B, Toutain A, Berard C, Vaksmann G, Weber S, Becane H-M, Perindopril preventive treatment on mortality in Duchenne muscular dystrophy: 10 years' follow-up., Am. Heart J 154 (2007) 596–602. doi:10.1016/j.ahj.2007.05.014. [PubMed: 17719312]

[101]. Bangalore S, Fakheri R, Toklu B, Ogedegbe G, Weintraub H, Messerli FH, Angiotensin-Converting Enzyme Inhibitors or Angiotensin Receptor Blockers in Patients Without Heart Failure? Insights from 254,301 Patients from Randomized Trials, Mayo Clin. Proc 91 (2016) 51–60. doi:10.1016/j.mayocp.2015.10.019. [PubMed: 26763511]

[102]. Pitt, Poole-Wilson PA, Segal R, Martinez FA, Dickstein K, Camm AJ, Konstam MA, Riegger G, Klinger GH, Neaton J, Sharma D, Thiyagarajan B, Effect of losartan compared with captopril on mortality in patients with symptomatic heart failure: randomised trial - the Losartan Heart Failure Survival Study ELITE II, Lancet. 355 (2000) 1582–1587. doi:10.1016/S0140-6736(00)02213-3. [PubMed: 10821361]

Highlights:

- Adrenergic stimulation extensively damages dystrophin-deficient hearts.
- Isoproterenol injection results in clinically-relevant dystrophic heart injury.
- Damaged dystrophic myocardium shows exaggerated and prolonged immune infiltration.
- Acute losartan prevents myocardial injury induced by isoproterenol in mdx mice.
- Losartan treatment modulates immune cell infiltration following myocardial injury.

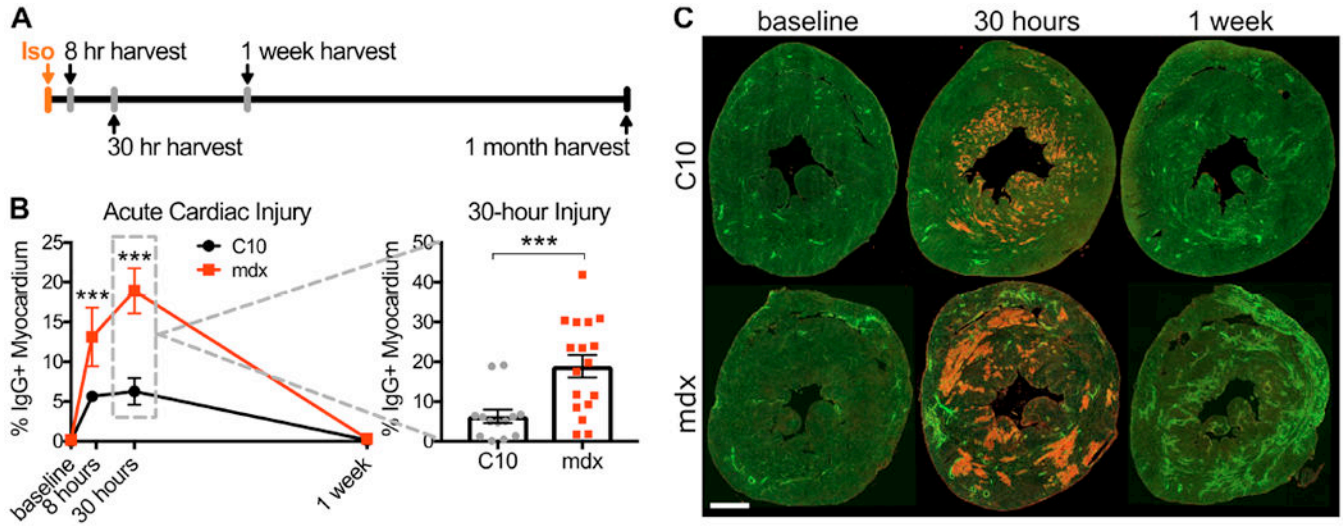

Figure 1: Effects of a single dose of isoproterenol on healthy and dystrophic hearts.

(A) After one bolus injection of 10 mg/kg isoproterenol (Iso), mice were sacrificed at timepoints of 8 hours, 30 hours, 1 week, or 1 month. (B) *Left:* Acute Iso-induced injury, measured by IgG incorporation, was prevalent as early as 8 hours, with a peak at 30 hours. Evidence of acute injury was totally removed by 1 week. (*** indicates p<0.001 vs. baseline; interaction p=0.01; n = 6-17 mice per group). *Right:* Wild type (C10) hearts displayed a peak acute injury area of only 6±2%, while mdx peak injury was 3-fold higher at 19±3%. (*** indicates p<0.001). (C) Representative images of data shown in panel B. Whole hearts are shown with WGA (green) marking the total tissue area and IgG (red) indicating areas of acute myocyte injury. Scale bar = 1mm.

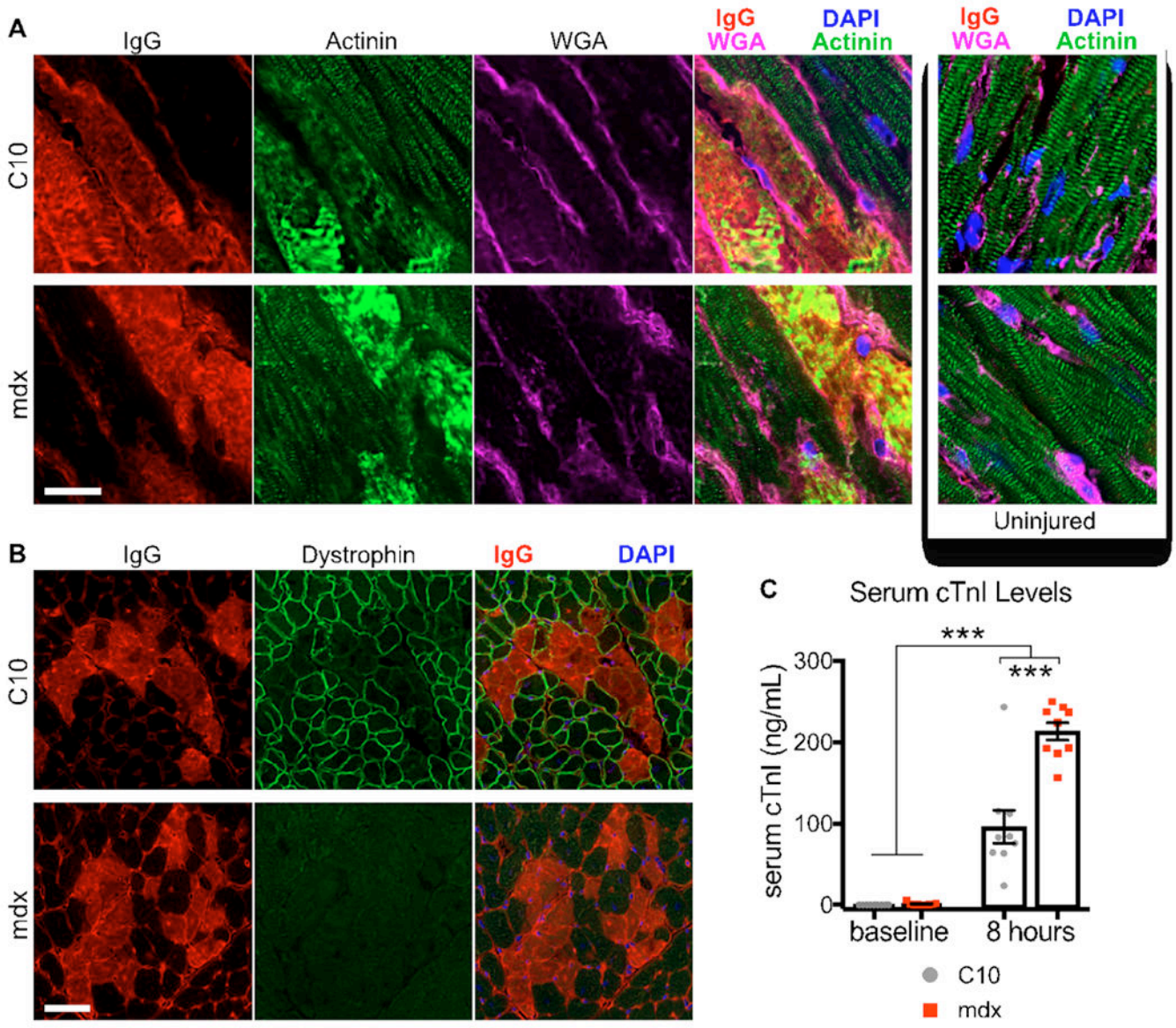

Figure 2: Sarcolemmal injury triggers cardiomyocyte destruction as early as 8 hours after Iso.

(A) In both wild type (C10) and dystrophic hearts, uptake of IgG into injured myocytes corresponds with profound disruption of sarcomere structure as early as 8 hours following a bolus of Iso, compared to uninjured cardiomyocyte sarcomeres (right). Sarcomeres were visualized by α-actinin staining (green), myocyte injury was marked by endogenous IgG uptake (red), and extracellular matrix was visualized by WGA staining (magenta). Scale bar = 20 μm. (B) In wild type mouse hearts, myocytes that had taken up IgG also lost dystrophin at the sarcolemma, evidenced by absence of dystrophin staining (green). As expected, mdx hearts did not exhibit dystrophin staining. Scale bar = 50 μm. (C) Cardiac troponin I (cTnI) concentration was measured in serum collected from wild type and mdx mice as an index of myocardial damage. Dystrophic mice showed significantly higher serum levels of cTnI 8 hours after Iso. (*** indicates $p<0.001$; $n \geq 8$ mice per group).

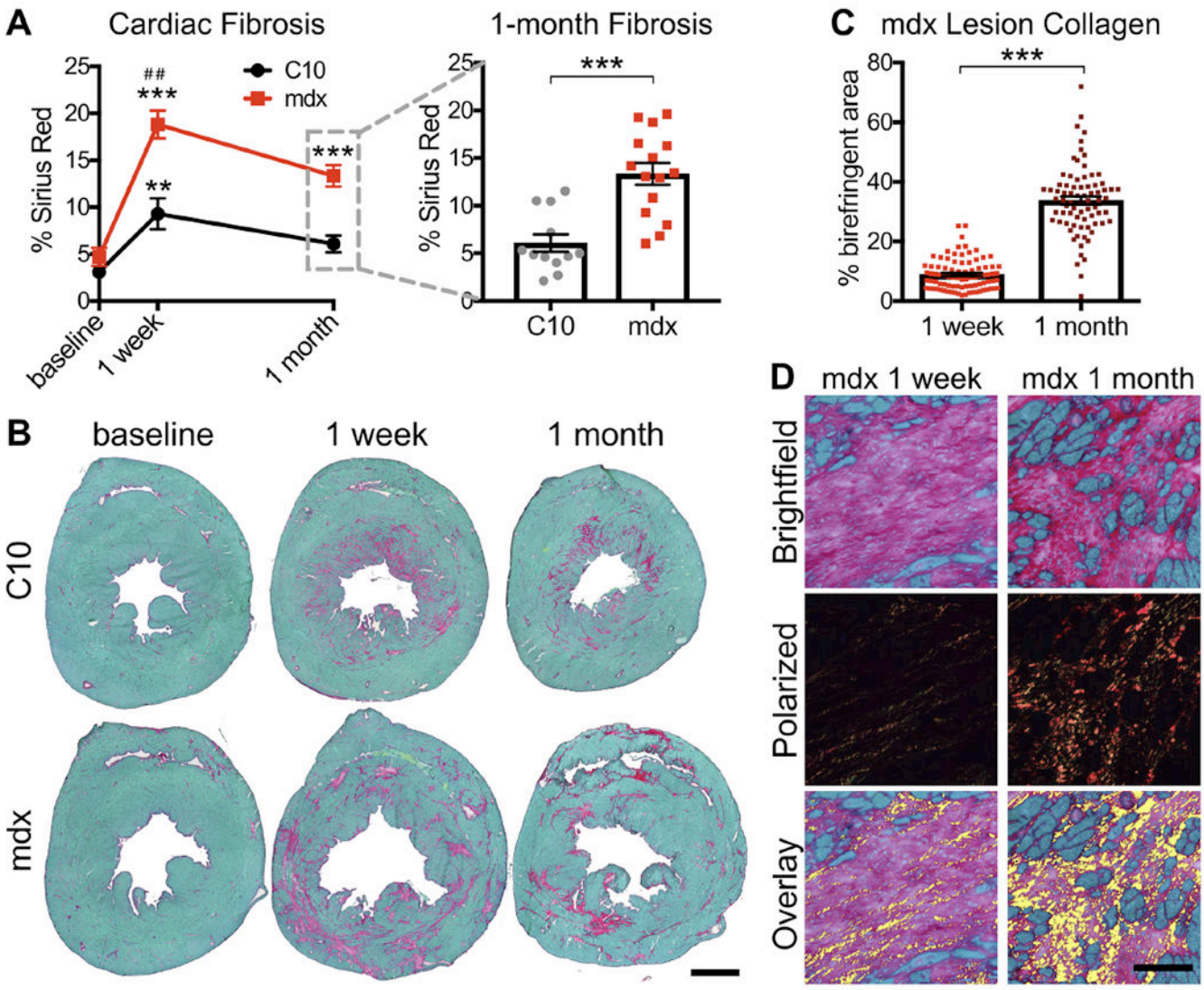

Figure 3: Fibrotic replacement of Iso-induced cardiac injury is dynamic.

(A) *Left:* In wild type and dystrophic hearts, the area of fibrosis was the highest 1 week after Iso-induced injury, and declined by 1 month (** indicates p=0.009 vs. baseline, *** indicates p<0.001 vs. baseline, ## indicates p=0.003 vs. 1 month; interaction p=0.02; n = 8-15 mice per group). *Right:* One month after injury, mdx hearts displayed significantly larger fibrotic area (13±1%) than control hearts (6±1%) (*** indicates p<0.001). (B) Representative montages of data displayed in panel A. Whole hearts are shown with Fast Green-stained myocardium and Sirius Red-stained fibrosis. Scale bar = 1mm. (C) One month after Iso-induced injury, fibrotic lesions in mdx hearts displayed dramatically increased birefringent area relative to 1-week lesions, suggesting that replacement fibrosis contracts during maturation. (*** indicates p<0.001, n = 76-86 lesions from 14 mice per group). (D) Representative images of data displayed in panel C. Matched brightfield, cross-polarized, and overlay images of mdx hearts show the change in the birefringence of 1-week and 1-month-old lesions; areas of birefringence are denoted in yellow on overlay images. Scale bar = 100 μm.

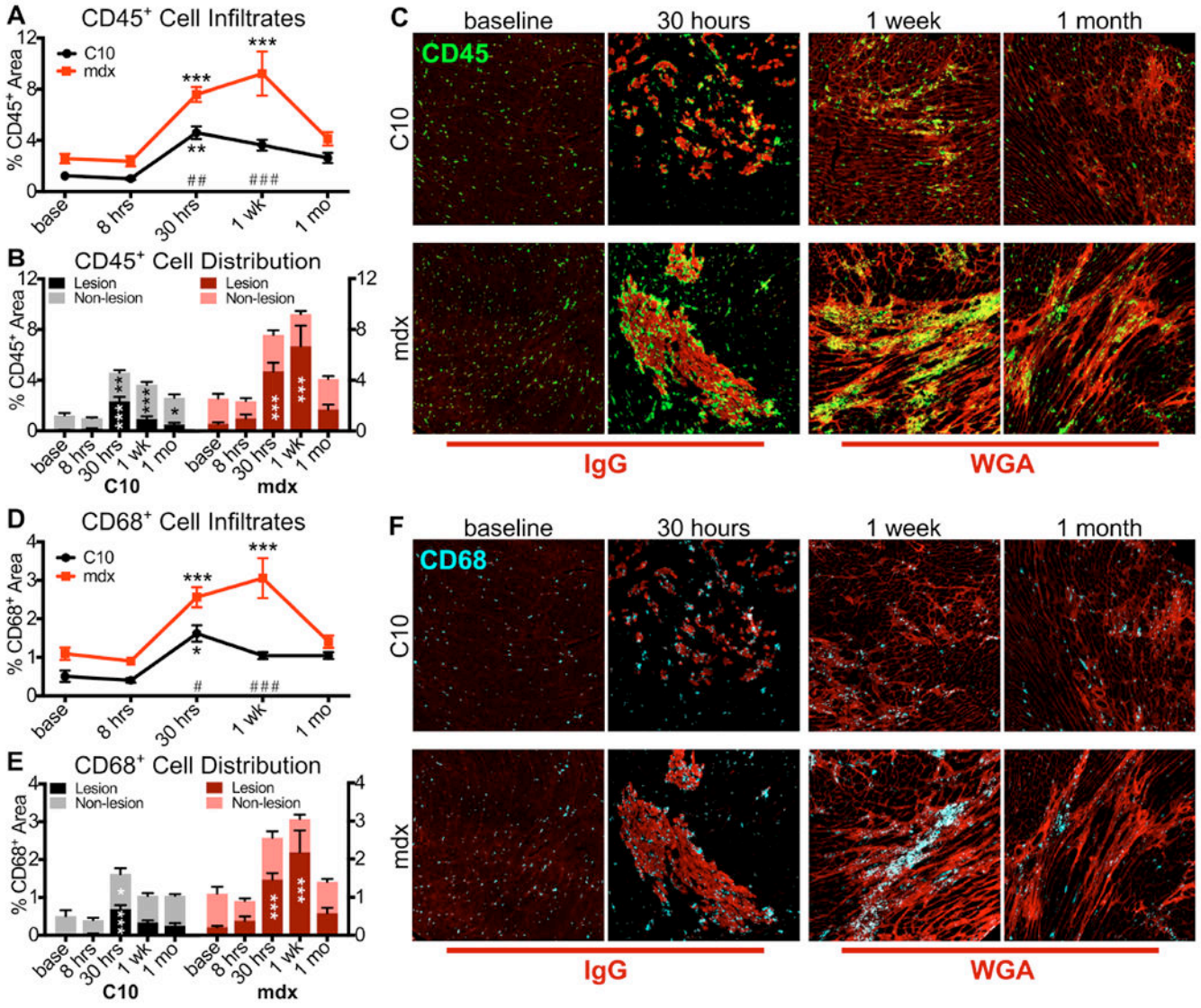

Figure 4: Iso-induced injury triggered a significantly greater immune cell response in dystrophic hearts.

(A) CD45$^+$ cell area was dramatically increased in mdx hearts 30 hours and 1 week after Iso administration, with a return toward baseline at 1 month after injury. Wild type (C10) hearts followed a similar pattern, with lower overall levels of infiltration and a faster return toward baseline levels (*** indicates p<0.001, ** indicates p=0.008 vs. baseline; ### indicates p<0.001, ## indicates p=0.004 difference between strains at the same timepoint; interaction p=0.02; n = 5-11 mice per group). (B) The expansion of the CD45$^+$ cell population occurred primarily in lesioned areas of the heart, where the CD45$^+$ area significantly increased compared to baseline in dystrophic hearts (*** indicates p<0.001, ** indicates p=0.008, * indicates p<0.05 vs. baseline). (C) Representative images for data shown in panels A and B. Cardiac lesions are represented by endogenous IgG uptake (red, baseline and 30 hours) and WGA accumulation (red, 1 week and 1 month). CD45$^+$ cells are shown in green. Each panel is 1 mm^2. (D) CD68$^+$ immune infiltrates were significantly increased in dystrophic hearts 30 hours and 1 week after Iso administration, with a return toward baseline by 1 month post-

injury. Wild type hearts displayed a smaller and shorter-lived surge in cardiac $CD68^+$ cells, with a significant increase observed only at 30 hours after Iso injection (*** indicates $p<0.001$, * indicates $p=0.02$ vs. baseline; ### indicates $p<0.001$, # indicates $p=0.01$ difference between strains at the same timepoint; interaction $p=0.02$; n = 4-12 mice per group). (E) $CD68^+$ cell expansion occurs primarily in lesioned areas of the heart, where their numbers are significantly greater compared to baseline. Only wild type hearts showed any expansion of non-lesion $CD68^+$ cell numbers at 30 hours after Iso injection (*** indicates $p<0.001$ vs. baseline, * indicates $p=0.02$ vs. baseline). (F) Representative images for data shown in panels D and E, with $CD68^+$ cells shown in cyan. Each panel is 1 mm^2.

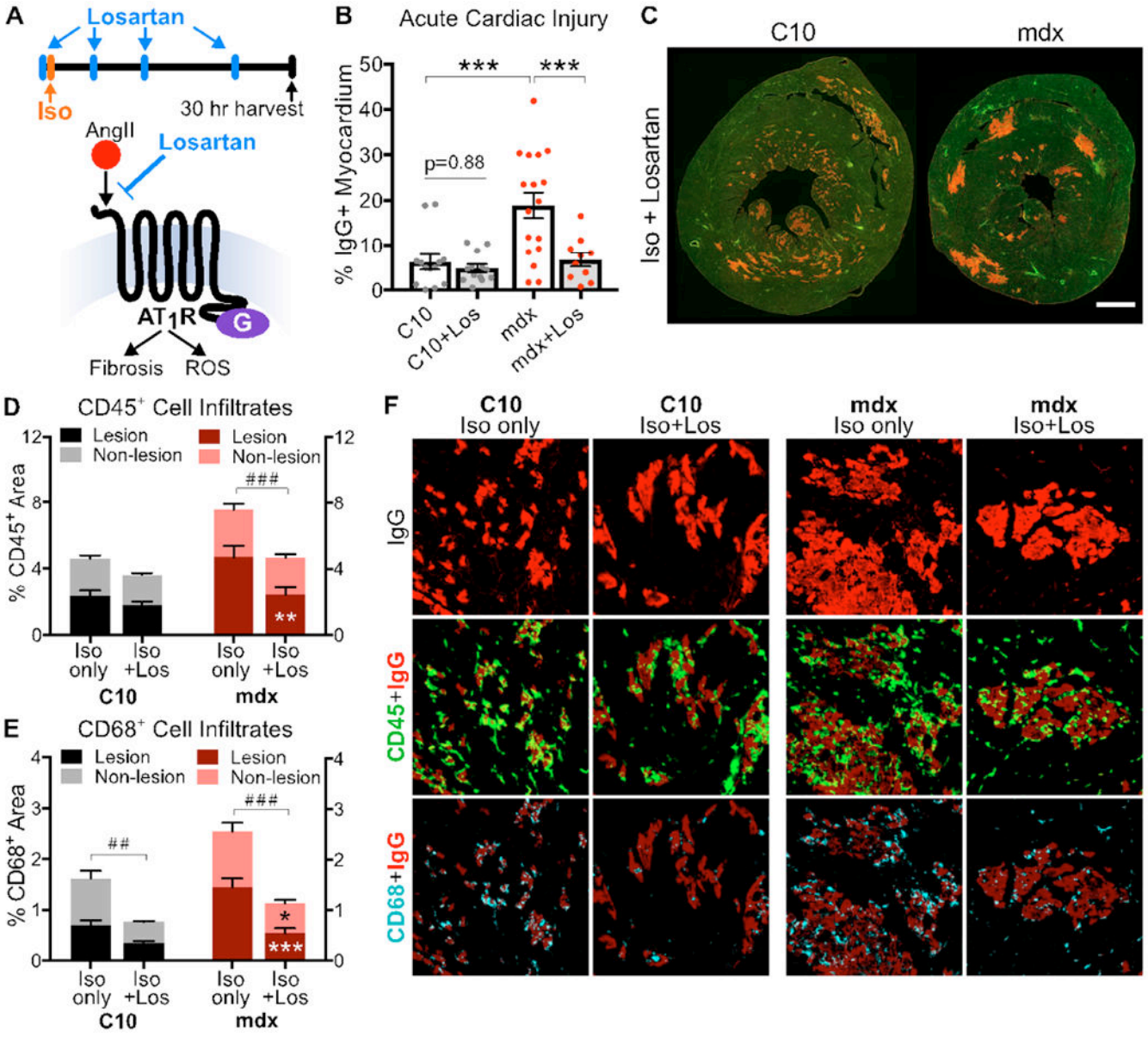

Figure 5: Acute losartan administration dramatically reduces Iso-induced injury in dystrophic hearts.

(A) Angiotensin II type 1 receptors (AT_1R) are G protein-coupled receptors that can be activated by angiotensin II (Ang II) and blocked by losartan. *Top:* Mice were treated with bolus injections of losartan (green) 1 hour prior to Iso administration (red), and at regular intervals over 30 hours following Iso injection. (B) 30 hours after Iso, losartan treatment caused no significant change in wild type (C10) cardiac injury, resulting in similarly low levels of acute Iso-induced injury in wild type and dystrophic hearts with losartan treatment. Untreated C10 and mdx data originally presented in Fig. 1B, shown here for comparison. (*** indicates $p<0.001$; interaction $p=0.02$; n = 10-17 mice per group). (C) Representative images of data shown in panel B. Whole hearts are shown with WGA (green) marking the total tissue area and IgG (red) indicating areas of acute myocyte injury. Scale bar = 1mm. (D

and E) $CD45^+$ and $CD68^+$ areas with and without losartan in wild type and mdx hearts, in both lesion and non-lesion areas. (*** indicates $p<0.001$, ** indicates $p<0.01$, * indicates $p=0.03$ vs. same domain without losartan; ### indicates $p<0.001$, ## indicates $p<0.01$ difference in total immune area; $n = 9$-13 mice per group). (F) Representative images for data shown in panels D and E, with $CD45^+$ cells shown in green and $CD68^+$ cells shown in cyan. Cardiac lesions are indicated by endogenous IgG uptake (red). Each panel is 0.25 mm^2.